Polyamide Solid State Polymerization: Evaluation of Pertinent Kinetic Models

S. N. Vouyiouka,[1] C. D. Papaspyrides,[1] J. Weber,[2] D. Marks[2]

[1]*Laboratory of Polymer Technology, School of Chemical Engineering, National Technical University of Athens, Zographou, Athens 157 80, Greece*
[2]*Experimental Station, INVISTA, Inc., Wilmington, Delaware 19898*

Received 4 August 2004; accepted 15 December 2004
DOI 10.1002/app.21811
Published online in Wiley InterScience (www.interscience.wiley.com).

ABSTRACT: Nylon 6,6 resins, in the form of pellets, were solid state polymerized in the temperature range of 160–200°C in a fixed-bed reactor under flowing nitrogen for times of 0–4 h. The kinetics of the solid state polymerization (SSP) of nylon 6,6 were examined by the evaluation of pertinent rate expressions and the selection of the most suitable one for describing the apparent overall process. The Flory-theory-based kinetic models were the most effective both for this study's data and for data previously published on SSP of different polyamides. Accordingly, SSP rate constants and activation energies were derived, and process parameters, such as the temperature and time, were investigated. © 2005 Wiley Periodicals, Inc. J Appl Polym Sci 97: 671–681, 2005

Key words: activation energy; kinetics (polym.); nylon; solid-state polymerization

INTRODUCTION

Polyesters and polyamides (PAs) are commercially important polymers prepared by polycondensation through melt polymerization. The products often have a lower-than-desired molecular weight because of problems arising from the increase in the melt viscosity and the removal of byproduct water or glycol.[1,2] Higher molecular weights may be reached through solid state polymerization (SSP) at temperatures between the glass transition and the onset of melting.[3–11] Polycondensation progresses through chain-end reactions in the amorphous phase of semicrystalline polymers,[12,13] which in most cases are flakes or powder. Reaction byproducts are removed by the application of vacuum or by the passage of an inert gas through the polymer.[8,10]

The rate of SSP involves both chemical and physical steps because it is controlled by intrinsic reaction kinetics, reactive chain-end mobility, and condensate removal through diffusion. Each of these steps may determine the rate-controlling mechanism under certain SSP conditions.[14–16] The reaction temperature emerges as the most important parameter of the SSP rate variation because of its interaction with all aspects of the process.[14,17,18] A higher prepolymer molecular weight leads to an increase in the SSP rate because it is accompanied by elevated degrees of crystallinity; this implies more effective confinement of the amorphous phase and, therefore, a high concentration and homogeneous distribution of reactive chain ends.[16,19,20] Also, a reduction in the polymer particle size with higher inert gas flow rates increases the effectiveness of byproduct removal and results in an increase in the SSP rate.[21]

Two alternative approaches have been used to investigate SSP kinetics. The modeling approach emphasizes comprehensive or advanced models, based on assumptions regarding one or more controlling mechanisms. These models differ in the number of main and side chemical reactions considered, the number of controlling steps assumed, and the mathematical technique used. In the experimental approach, the SSP data treatment results in the determination of intrinsic or apparent rate constants through simple (empirical) models, which consider only the main chemical reactions. The effects of different variables on the SSP rate are also investigated to determine the rate-controlling mechanism. In this article, emphasis is given to the experimental approach. Accordingly, the already developed kinetic models may be classified into two groups: the Flory-theory-based models and the power-of-the-time models. These rate expressions are presented in Table I and are analyzed in the following sections.

Flory-theory-based models

According to Flory's theory,[22] the polycondensation rate can be described by second- or third-order (auto-

Correspondence to: C. D. Papaspyrides (kp@softlab.ece.ntua.gr).

TABLE I
Published SSP Rate Expressions

Approach	Rate expression
Flory-theory-based models	
Equation (1)[16]	$(n-1)\log\left(\sqrt[a]{\left(\frac{1}{\sqrt{P_t}}\right)^a-\left(\frac{1}{\sqrt{P_0}}\right)^a}\right)-\log(n-1)k=\log t$
	k = rate constant [(kg/mequiv)$^{n-1}$ h^{-1}]
	n = reaction order
	a = chosen as near as possible to $n-1$
	P = [—COOH][—NH_2]
Equation (2)[24]	$(M_n)^{n-1}-(M_{n_0})^{n-1}=(n-1)kt$
	k = rate constant [(g/mol)$^{n-1}$ h^{-1}]
	n = reaction order
Equation (3)[25]	$M_n=M_{n_0}+k\sqrt{t}$
	k = rate constant [(g/mol) h$^{-0.5}$]
Equation (4)[15,26]	$\frac{[C]_0-[C]_t}{t}=2k_a([C]_0-[C_{ai}])[C]_t-2k_a([C]_0-[C_{ai}])[C_{ai}]$
	$[C]_0$ = initial total end-group concentration (mequiv/kg)
	$[C]_t$ = total end-group concentration at any given time (mequiv/kg)
	$[C_{ai}]$ = constant apparent inactive end-group concentration (mequiv/kg)
	k_a = apparent second-order rate constant [(kg/mequiv) h^{-1}]
Flory-theory-based models: Two-phase model	
Equation (6)[29]	$(M_n)^{n-1}-(M_{n_0})^{n-1}=\frac{n-1}{(1-x_c)^{n-1}}kt$
	k = rate constant [(g/mol)$^{n-1}$ h^{-1}]
	n = reaction order
	x_c = mass fraction crystallinity
Power of the time models	
Equation (8)[32]	$\ln(M_n-M_{n_0})=\ln\left(\frac{k}{n+1}\right)+(n+1)\ln t$
	k = rate constant [(g/mol) h^{-n-1}]
	n = power of the time
Equation (9)[19]	$\ln\left(-\frac{d[\mathrm{COOH}]}{dt}\Big/[\mathrm{COOH}]\right)=\ln k+n\ln t$
	k = rate constant (h^{-n-1})
Equation (10)[33]	$\mathrm{RV}={}_tRV_0+\frac{k}{n+1}t^{n+1}$
	k = rate constant (h^{-n-1})
	n = power of the time

catalyzed reaction) expressions of functional end groups, under the assumption of equal reactivity. This principle is most accurate during the final stages of polymerization and also in prepolymer SSP, for which the very early stages of polymerization are excluded.[23] Many different, but almost equivalent, sets of integrated equations have been developed by several researchers to describe Flory's theory, and they are presented next with respect to the irreversible SSP reaction.

Gaymans[16] studied the SSP of unbalanced poly(tetramethylene adipamide) (PA4,6) and proposed a kinetic expression in terms of the product of the concentrations of the end groups (P) and the reaction order [n; eq. (1), Table I]. According to Srinivasan et al.,[24] if a stoichiometric equivalence is assumed in the poly(hexamethylene adipamide) (PA6,6) prepolymer, the reaction rate can be expressed through the number-average molecular weight [M_n; eq. (2), Table I]. In addition, Jabarin and Lofgren[25] used eq. (3) (Table I), which relates M_n during SSP to the square root of time. Alternatively, the kinetic model by Duh[15,26] [eq. (4), Table I] is based on the assumption that two categories of end groups exist during poly(ethylene terephthalate) (PET) SSP: active and inactive ones. It has been suggested that the overall SSP follows second-order kinetics and that the proposed rate equation involves the apparent reaction rate constant and the constant apparent inactive end-group concentration, which decreases linearly with the SSP temperature. Such a rate expression has been proposed to be adequate in cases in which SSP is jointly controlled by reaction and end-group diffusion.

The SSP kinetic models may be transformed to take into consideration the two-phase model, as suggested by Zimmerman.[12,13] The end groups and low-molec-

ular-weight substances (condensate and oligomers) are exclusively in the amorphous regions, in which the equilibrium is the same as that for a completely amorphous or molten polymer at the same temperature. Accordingly, the concentrations of the end groups involved in the SSP reaction should be corrected properly as follows:[12,27,28]

$$[C_{\text{amorphous}}] = \frac{[C_{\text{overall}}]}{1 - x_c} \quad (5)$$

where $[C_{\text{amorphous}}]$ is the concentration of end groups in the amorphous phase of the polymer (mequiv/kg), $[C_{\text{overall}}]$ is the concentration of end groups in the total mass of the polymer (mequiv/kg), and x_c is the mass fraction crystallinity.

The two-phase model has been used in the study of the SSP of PA6,6 fibers.[29] A rate expression [eq. (6), Table I], based on eq. (2) (Table I), has been developed in terms of n, M_n, and x_c.

Power-of-the-time models

Turning to the power-of-the-time models proposed, various researchers have tried to compile empirical equations, implying that the diffusion process predominates also in the overall SSP reaction.[30] A widely used pertinent equation is that of Walas,[31] who pointed out that the rate of a process in a solid material, which is controlled by the chemical reaction and diffusion, usually varies as some power n of the time:

$$\text{Rate} = kt^n \quad (7)$$

Griskey and Lee[32] used a modified form of Walas's equation, in which M_n in SSP varies as some power n of the time [eq. (8), Table I]. Gaymans et al.[19] suggested that the process is limited by the diffusion rate of the autocatalyzing acid end and that this is dependent not only on its concentration and the temperature but also on the changing end-group-to-end-group distance distribution. Therefore, they developed a kinetic expression, which associates the rate of the reaction with the concentration of the catalyzing end groups [COOH] and with some power n of time [eq. (9), Table I], thus combining the Flory theory with the Walas equation. Finally, during their study of PA6,6 SSP, Fujimoto et al.[33] formulated a rate equation in which the relative viscosity (RV) increases as some power of the time [eq. (10), Table I]. In Table II, the values of the rate constants and the SSP activation energy (E_a) are presented for the pertinent kinetic models.

In this article, a simple Flory-based SSP kinetic model is used, which, together with the aforementioned rate expressions, is evaluated for fitting our PA6,6 SSP data and previously published SSP data for different PAs. This effort is of significant interest because there is no universal agreement on the relevant kinetic models, and it will be feasible to obtain apparent rate constants. A reliable rate equation for describing the SSP reaction is needed, especially because the forward reaction rate constants used in SSP comprehensive models are usually extrapolated from melt polymerization data despite the very different morphology of the solid polymer. Finally, pertinent studies are focused mainly on PET SSP kinetics,[15] whereas the amount of published data on polyamide SSP is quite limited.

EXPERIMENTAL

Starting material

PA6,6 was supplied by INVISTA, Inc. (Wilmington, DE). The prepolymer was prepared by the melt polymerization of aqueous nylon 6,6 salt and contained no additives. The samples were in the form of flakes, and before any SSP runs, they were sieved and dried *in vacuo* (80°C, 4 h). The particle size selected for the SSP runs was 10–12 mesh (1.7–1.4 mm).

SSP runs

A bench scale reactor, assembled by INVISTA, with a 50-g resin capacity, was used to solid state polymerize the PA6,6 prepolymer under various time and temperature conditions (Table III). The cylindrical, stainless steel reactor was equipped with a gas inlet below the sample chamber to permit preheated purge gas [nitrogen (N_2)] to pass through the polymer bed during the reaction. The purge gas was used to distribute heat evenly throughout the sample chamber and to remove volatile reaction products. The nitrogen, controlled at a constant predetermined flow rate (260 mL/min) through a calibrated rotometer, was preheated while passing through a coil of 1/8-in. stainless steel tubing. Thermocouples at two individual locations within the reaction chamber were used to monitor the polymer temperature during SSP. A fluidized sand bath (Techne Corp., Minneapolis, MN) was used to heat the reactor and the purge gas. Four heating elements heated the sand, fluidized by air, to the SSP temperatures.

The reactor was first filled with dried and sieved prepolymer (30 g), closed, and examined for leaks through a pressure test. It was then left overnight under a constant nitrogen flow (18 mL/min) to remove oxygen. The temperature of the sand bath was raised to the SSP temperature (T_R), and the reactor, under continued nitrogen flow, was immersed in the fluidized bath. The time required to reach T_R in the interior of the reactor was measured, and the experiment was considered to begin from the point at which

TABLE II
Reaction Kinetic Data Related to the Irreversible SSP of Polymers

	Starting material	Operating conditions	Rate constant (k)	E_a (kcal/mol)
Griskey and Lee[32]	PA6,6 (d_{mean} = 0.18 cm)	90–135°C, 0–10 h, N_2	$k = 1.53 \times 10^{10} \exp(-12{,}960/RT)$ ($h^{-0.51}$)	13.0
Chen et al.[34]	PA6,6 (d_{mean} = 0.35–0.20 cm)	120–180°C, 5–20 h, N_2	$k = 1.39 \times 10^{4} \exp(-10{,}500/RT)$ ($h^{-0.5}$)	10.5
	PA6, 10 (d_{mean} = 0.22–0.34 cm)	120–180°C, 5–20 h, N_2	$k = 1.68 \times 10^{4} \exp(-13{,}200/RT)$ (h^{-1})	13.2
Fujimoto et al.[33]	PA6,6 (d_{mean} = 0.3 cm)	160–210°C, 0–80 h, N_2	$\log k = 13.8 - \frac{5.90 \times 10^3}{T}$ (h^{-1})	26.0
Srinivasan et al.[24]	PA6,6 fibers	220–250°C, 0–4 h, N_2	$k = 6.29 \times 10^{40} \exp(-76{,}000/RT)$ [$(g/mol)^2\ s^{-1}$]	76.0
Srinivasan et al.[29]	PA6,6 fibers	220–250°C, 0–4 h, N_2	Second order	
			$k = 3.06 \times 10^{18} \exp(-42{,}000/RT)$ [$(g/mol)\ s^{-1}$]	42.0
			Third order	
			$k = 1.18 \times 10^{31} \exp(-61{,}000/RT)$ [$(g/mol)^2\ s^{-1}$]	61.0
Gaymans et al.[19]	PA6 (d_{mean} = 0.02–0.05 cm)	110–205°C, 1–24 h, N_2	For conversions > 30%, $k = 0.28$	
Chen et al.[34]	PET (d_{mean} = 0.10–0.21 cm)	160–200°C, 5–20 h, N_2	$k = 6.6 \times 10^{17} \exp(-42{,}500/RT)$ (h^{-1})	42.5
Jabarin and Lofgren[25]	Commercial PET (Goodyear VFR-6014, Firestobe A, Eastman 7328)	200–250°C, 0–16 h, N_2	Catalytic reaction	
			Goodyear VFR-6014 $k = 624 \times 10^{10} \exp(-22{,}800/RT)$	18.4–23.2
			Firestobe A $k = 828 \times 10^{10} \exp(-23{,}200/RT)$	
			Eastman 7328 $k = 5.70 \times 10^{10} \exp(-18{,}400/RT)$ [$(g/mol)\ min^{-0.5}$]	

d_{mean} = mean diameter.

the reactor interior temperature was T_R. After heating for a predetermined period of time, the reactor was cooled (<40°C), and the product was removed from the reactor vessel, placed in a plastic container, sealed, and stored in a desiccator.

In the following results, the SSP products are named first by the starting material, second by the reaction temperature, and third by the reaction time.

PA characterization

The PA6,6 prepolymer and the SSP products were analyzed to determine the end-group contents, RVs, molecular weight distributions (MWDs), and melting–crystallization characteristics. The reproducibility of the results was estimated from the values of the standard deviation of the mean (SDM).

TABLE III
Experimental Conditions of the PA6,6 SSP Runs

	Times (h) for an SSP reaction temperature of		
Inert gas	160°C	180°C	200°C
Nitrogen, flowing	0, 1, 2, 3, 4	0, 2, 4	0, 2, 4

End-group analysis

The end-group concentrations were determined by potentiometric titration. For amine end determination, the samples were dissolved in a mixture of 85% phenol and 15% methanol and titrated with a solution of perchloric acid in methanol. For acid end analysis, the polymer was dissolved in a 5:1 mixture of *o*-cresol/5% *o*-dichlorobenzene and 20% LiCl/methanol and was titrated with a solution of tetrabutyl ammonium hydroxide in benzyl alcohol.

Viscosity measurements

The RV of PA6,6 was the ratio of the viscosity of a solution of 8.4 wt % polymer in a solution of 90% formic acid to the viscosity of the formic acid solution. The viscosity measurements were performed with a Cannon-Fenske (State College, PA) viscometer at 25°C.

MWD

The samples were dissolved in 1,1,1,3,3,3-hexafluoro-2-propanol (HFIP) with 0.01*M* sodium trifluoroacetate and then were analyzed by size exclusion chromatography (SEC), with an Alliance 2690 system (Waters Corp., Milford, MA).

Differential scanning calorimetry (DSC)

The DSC analysis was performed in the range of 30–300°C at a heating rate of 10°C/min. The system used was a PerkinElmer (Wellesley, MA) DSC 4.

RESULTS AND DISCUSSION

Theoretical

The main difference between melt polymerization and SSP is the difficulty of the segmental mobility of the polymer chains during SSP and thus of the end-group diffusion limitations, which do not exist in the melt.[13] The overall SSP process may be divided into two stages. In the first stage, the distribution of end groups in the solid polymer is homogeneous as in the case of the melt process, and consequently, the reaction kinetics and mechanisms will be similar. The end groups with the smallest end-to-end distances do not need to diffuse to react, and the reaction rate constant is the intrinsic rate constant. In the second stage, the diffusion of polymer chain ends starts to be the limiting step, and the reaction rate is strongly affected by end-group diffusion limitations. The latter results, in many cases, in reducing the apparent reaction rate constant,[2,35,36] and for this reason, an asymptotic value of the molecular weight is reached at long reaction times.[35,37,38] Therefore, in this analysis, short SSP reaction times (0–4 h; Table III) have been selected to prevent SSP retardation due to end-group diffusion limitations.

On the basis of the aforementioned considerations, Flory's equations for second and third reaction orders can be integrated as follows:

$$-\frac{d[\mathrm{COOH}]}{dt} = k_2[\mathrm{COOH}][\mathrm{NH_2}] \Rightarrow \frac{dx}{dt} = k_2([\mathrm{COOH}]_0 - x)([\mathrm{NH_2}]_0 - x) \quad (11)$$

$$-\frac{d[\mathrm{COOH}]}{dt} = k_3[\mathrm{COOH}]^2[\mathrm{NH_2}] \Rightarrow \frac{dx}{dt} = k_3([\mathrm{COOH}]_0 - x)^2([\mathrm{NH_2}]_0 - x) \quad (12)$$

where x is the concentration of the reacted groups (mequiv/kg), $[\mathrm{COOH}]_0$ and $[\mathrm{NH_2}]_0$ are the initial concentrations of the carboxyl and amine end groups (mequiv/kg), and k_2 [(kg/mequiv)h^{-1}] and k_3 [(kg/mequiv)^2 h^{-1}] are the rate constants for second- and third-order kinetics.

In the case of carboxyl end-group excess in the prepolymer, the polymerization conversion (p_t) is calculated at any given reaction time on the basis of the amine group concentrations. The integration ($t = 0$, $p_0 = 0$) of the aforementioned equations results in the rate expressions A_2 (kg/mequiv) and A_3 (kg^2/mequiv^2) for the second and third orders, respectively:

$$A_2 = \frac{1}{D_0}\left(\ln\frac{1}{[\mathrm{COOH}]_0} + \ln\frac{[\mathrm{COOH}]_0 - [\mathrm{NH_2}]_0 p_t}{1 - p_t}\right) = k_2 t \quad (13)$$

$$A_3 = \frac{1}{D_0^2}\ln\frac{[\mathrm{COOH}]_0 - [\mathrm{NH_2}]_0 p_t}{[\mathrm{COOH}]_0(1 - p_t)} - \frac{1}{D_0}\left(\frac{1}{[\mathrm{COOH}]_0 - [\mathrm{NH_2}]_0 p_t} - \frac{1}{[\mathrm{COOH}]_0}\right) = k_3 t \quad (14)$$

where D_0 is the initial carboxyl end-group excess (mequiv/kg). For amine end-group excess, eqs. (11) and (12) are integrated on the basis of the polymerization conversion of the carboxyl end groups, and this results in similar expressions.

The concentrations $[\mathrm{COOH}]_0$ and $[\mathrm{NH2}]_0$ refer to values for the polymer phase as a whole, not only in the amorphous regions. To include the variation of the crystallinity with time, eq. (5) can be used, and the resulting rate expressions are in fact eqs. (13) and (14) multiplied by the factor $(1 - x_c)^{n-1}$, where n is the reaction order. For instance, in second-order kinetics, the rate expression becomes

$$\frac{1 - x_c}{D_0}\left(\ln\frac{1}{[\mathrm{COOH}]_0} + \ln\frac{[\mathrm{COOH}]_0 - [\mathrm{NH_2}]_0 p_t}{1 - p_t}\right) = k_2 t \quad (15)$$

Evaluation of the kinetic models

All rate expressions discussed so far have been tested and compared by the fitting of our experimental data at a single reaction temperature (160°C; Table III). The latter has been chosen to be relatively low to minimize byproduct diffusion limitations and to focus on reaction intrinsic kinetics. The SSP data used are presented in Table IV, in which the carboxyl end-group excess (D), the fractional conversion (p_t), and M_n are also listed. The application of the kinetic models has led to values of the rate constants at any given reaction time; on this basis, a mean value (k_{mean}) has been determined (Table V). SDM has also been calculated and indicates the model fitting. In addition, the rate constants have been derived from the slope of the lines (k_{plot}) of the rate expressions versus the reaction time,

TABLE IV
PA6,6 SSP Data at 160°C

	SSP time (h)	x_c (%)	RV	$[NH_2]$ (mequiv/kg)	[COOH] (mequiv/kg)	D (mequiv/kg)	M_n (g/mol)	p_t
PA6,6			64.2 ± 0.05	48.9 ± 0.2	69.1 ± 0.3	20.1	17,000	
PA1600	0.0	26	65.8 ± 0.04	46.8 ± 0.1	68.7 ± 0.2	21.9	17,300	0.000
PA1601	1.2		67.0 ± 0.08	45.5 ± 0.2	72.3 ± 0.7	26.8	17,000	0.028
PA1602	2.0		82.1 ± 0.03	43.6 ± 0.3	67.4 ± 0.8	23.8	18,000	0.068
PA1603	3.1		83.6 ± 0.06	42.4 ± 0.4	68.7 ± 2.4	26.3	18,000	0.094
PA1604	4.2	25	90.7 ± 0.03	40.7 ± 0.2	62.7 ± 1.3	22.0	19,300	0.130

and the correlation coefficient (R^2) has been deduced. The deviation between k_{mean} and k_{plot} has also been calculated [$\Delta S^2 = (k_{mean} - k_{plot})^2$] and shows how well the model fits.

The Flory-based expression introduced by Gaymans,[16] eq. (1), does not successfully describe the SSP process. It leads to high SDM values (17–18%) and, more importantly, to significantly high values of ΔS^2. According to Gaymans, the SSP reaction does not follow third-order kinetics, but the apparent order varies between 3.5 and 5.2, as the SSP temperature decreases from 280 to 190°; this reveals that the apparent order increases with a lower reaction temperature. These SSP data have also been tested for n values of 5 and 6 in eq. (1), with consideration given to the low operating temperature (160°C), but the fit is still poor ($R^2 = 0.7461$ and 0.7450, respectively). A similar result has been observed with Srinivasan et al.'s[24] approach [eq. (2)]. The high deviation obviously results from the nonstoichiometric equivalence of the end groups in the prepolymer sample, which is, however, an assumption for the relevant kinetic expression. For the same reasons, eq. (3), introduced by Jabarin and Lofgren,[25] reveals a poor fit ($R^2 = 0.5311$). The Duh[15,26] model [eq. (4)] is completely inadequate. Finally, eqs. (13) and (14) present the lowest deviation (SDM = 8–9%) in comparison with the aforementioned kinetic models. The plots of the relevant rate expressions (A_2 and A_3) versus the reaction time (Fig. 1) are linear ($R^2 = 0.9883$–0.9894); they support the relevant kinetic model and allow the calculation of the rate constants from the line slopes (k_{plot}). A further indication of the good model fit is the low values of the deviation between k_{mean} and k_{plot} ($\Delta S^2 = 1 \times 10^{-9}$ to 1×10^{-12}).

TABLE V
Fitting SSP Data at 160°C to Different Kinetics Models

Equations	$100 \times k_{2mean}$ [(kg/mequiv) h^{-1}]	$1000 \times k_{3mean}$ [(kg/mequiv)^2 h^{-1}]	$100 \times k_{2plot}$ [(kg/mequiv) h^{-1}]	$1000 \times k_{3plot}$ [(kg/mequiv)^2 h^{-1}]	$\Delta S^2(k_2)$ [(kg/mequiv)^2 h^{-2}]	$\Delta S^2(k_3)$ [(kg/mequiv)^4 h^{-2}]
Flory-theory-based models						
(1) (t = 2, 3, and 4 h)	0.040 ± 17%	0.007 ± 18%	1.111 $R^2 = 0.7496$	0.208 $R^2 = 0.7484$	1×10^{-4}	4×10^{-8}
(2) (t = 2, 3, and 4 h)	0.035 ± 22%	0.006 ± 23%	0.043 $R^2 = 0.8085$	0.010 $R^2 = 0.7978$	6×10^{-9}	1×10^{-11}
(3): $M_n = 16{,}884 + 833.15\sqrt{t}$, $R^2 = 0.5311$, $k = 833.15$ [(g/mol) $h^{-0.5}$]						
(4): $\frac{C_0 - C_t}{t} = -0.3316C + 37.866$ (as derived, different from the model proposed)						
(13) and (14)	0.046 ± 8%	0.007 ± 9%	0.050 $R^2 = 0.9883$	0.008 $R^2 = 0.9894$	1×10^{-9}	1×10^{-12}
Flory-theory-based models: Two-phase model (x_c = 26%)						
(6) (t = 2, 3, and 4 h)	0.026 ± 22%	0.003 ± 23%	0.032 $R^2 = 0.8085$	0.055 $R^2 = 0.7978$	3×10^{-9}	3×10^{-9}
(15)	0.034 ± 8%		0.040 $R^2 = 0.9883$		3×10^{-9}	
Power of the time models						
(8) (t = 2, 3, and 4 h): $\frac{dM_n}{dt} = 303t^{0.3722}$ $R^2 = 0.6513$, $k = 303$ (g/mol) $h^{-1.3722}$						
(9): (t = 2 and 4 h): $-\frac{d[\text{COOH}]}{dt} = 0.004[\text{COOH}]t^{1.2358}$, $k = 0.004h^{-2.2358}$, poor fitting as negative rate constants were derived						
(10): $\frac{d\text{RV}}{dt} = 6.370$ $R^2 = 0.8953$, $k = 6.370h^{-1}$						

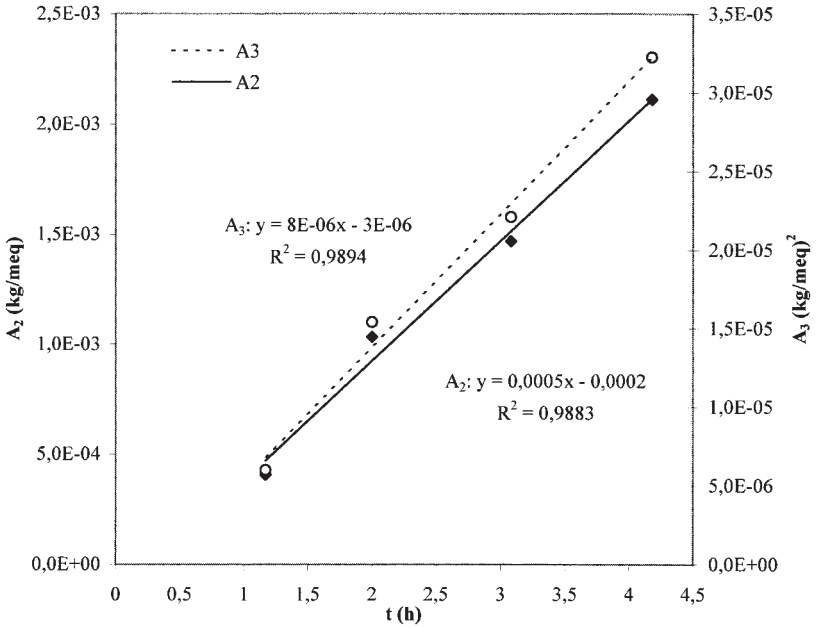

Figure 1 Fitting of rate expressions (♦) A_2 and (○) A_3 [eqs. (13) and (14)] versus the reaction time for the SSP of PA6,6 at 160°C.

The two-phase-model rate expression [eq. (6)][29] has the same SDM (22%) as eq. (2), as expected, because eq. (6) is in fact eq. (2) divided by $(1 - x_c)^{n-1}$, where n is the reaction order. The values of the rate constants are changed, but the deduced SSP E_a value is not affected.[35] Nevertheless, the crystallinity is constant through the SSP runs (Table IV), and thus the two-phase model does not need to be used in this analysis.

Regarding the power-of-the-time models, the Fujimoto approach [eq. (10)] shows a better fit to the experimental data and reveals the linearity of the RV values versus the reaction time, as found in a previous study.[33] However, such an expression serves only as a tool to get some idea of the rheological behavior of the polymer during SSP. According to Zimmerman and Kohan,[13] if the course of the reaction is followed by RV measurements rather than by end-group concentrations, the results may become confusing because of the possibility of branching reactions, since the viscosity will not usually increase as fast with increasing molecular weight for a branched chain as for a linear one. On the other hand, eq. (8) results in a low value of R^2 (0.6513), and the reaction order is 0.3722, deviating significantly from the findings of a previous study ($n = -0.49$).[32] As for eq. (9), the fit is very poor because some data lead to negative rate constants.

In conclusion, on the basis of the results in Table V, the Flory rate expressions fit better than the power-of-the-time models, revealing that the SSP rate depends primarily on the concentrations of the end groups under the specific experimental conditions; that is, the process is reaction-controlled. More spe-

TABLE VI
PA6,6 SSP Data at Three Reaction Temperatures

	SSP time (h)	RV	$[NH_2]$ (mequiv/kg)	[COOH] (mequiv/kg)	D (mequiv/kg)	M_n (g/mol)	$\Delta M_n/M_{n_0}$ (%)	p_t
160°C								
PA1600	0.0	65.8 ± 0.04	46.8 ± 0.1	68.7 ± 0.2	21.9	17,300		0.000
PA1602	2.0	82.1 ± 0.095	43.6 ± 0.3	67.4 ± 0.8	23.8	18,000	4	0.068
PA1604	4.2	90.7 ± 0.095	40.7 ± 0.21	62.7 ± 1.3	22.0	19,300	12	0.130
180°C								
PA1800	0.0	65.6 ± 0.02	44.3 ± 0.0	67.3 ± 1.5	23.0	17,900		0.000
PA1802	2.0	86.1 ± 0.00	37.7 ± 0.0	60.1 ± 0.4	22.4	20,400	14	0.149
PA1804	4.0	105.2 ± 0.09%	34.5 ± 0.0	59.2 ± 0.4	24.7	21,400	20	0.221
200°C								
PA2000	0.0	85.8 ± 0.01	40.4 ± 0.0	61.3 ± 0.5	20.9	19,700		0.000
PA2002	2.0	134.7 ± 0.19	30.6 ± 0.7	56.4 ± 1.0	25.8	23,000	17	0.243
PA2004	4.0	185.7 ± 0.05	26.7 ± 0.2	51.2 ± 1.2	24.5	25,700	31	0.339

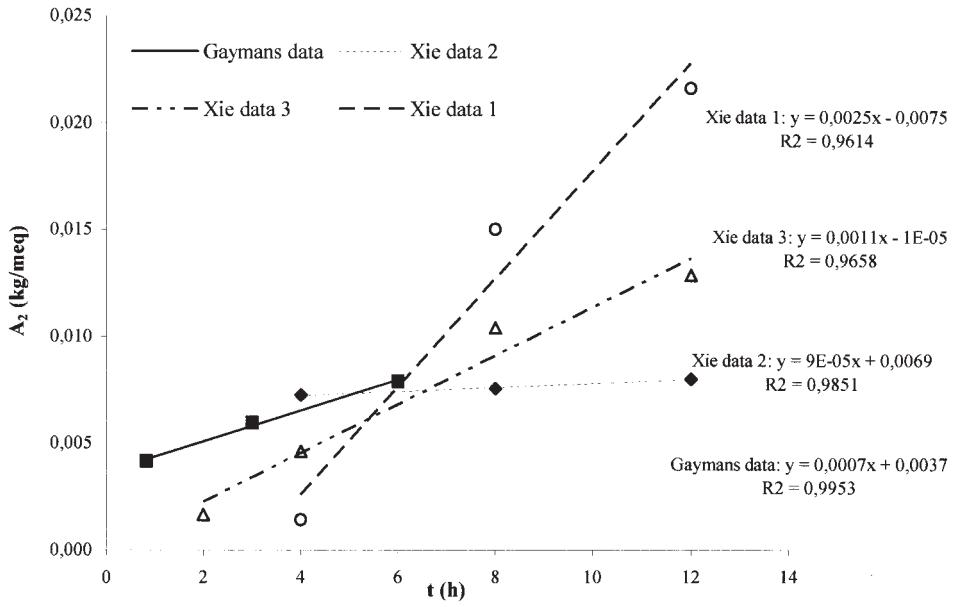

Figure 2 Fitting of rate expression A_2 to published SSP data for second-order kinetics: (■) Gaymans data (PA4,6, SSP temperature = 220°C), (○) Xie data 1 (PA6 chips with 0.03% regulator, SSP temperature = 200°C), (◆) Xie data 2 (PA6 chips, cylinder, mean diameter = 1.2 mm), and (△) Xie data 3 (PA6 chips, cylinder, mean diameter = 1.4 mm).

cifically, SSP is successfully described through eqs. (13) and (14), in which only the initial carboxyl end-group concentrations ($[COOH]_0$) are involved. The latter is really important because the —COOH analysis has lower reproducibility, and it is less accurate than —NH_2 determination (Tables IV and VI). The poor fit of the power-of-the-time models indicates that byproduct diffusion limitations may be disregarded. This observation may be attributed to the low reaction temperatures studied because byproduct diffusion limitations are generally predominant at much higher operating temperatures

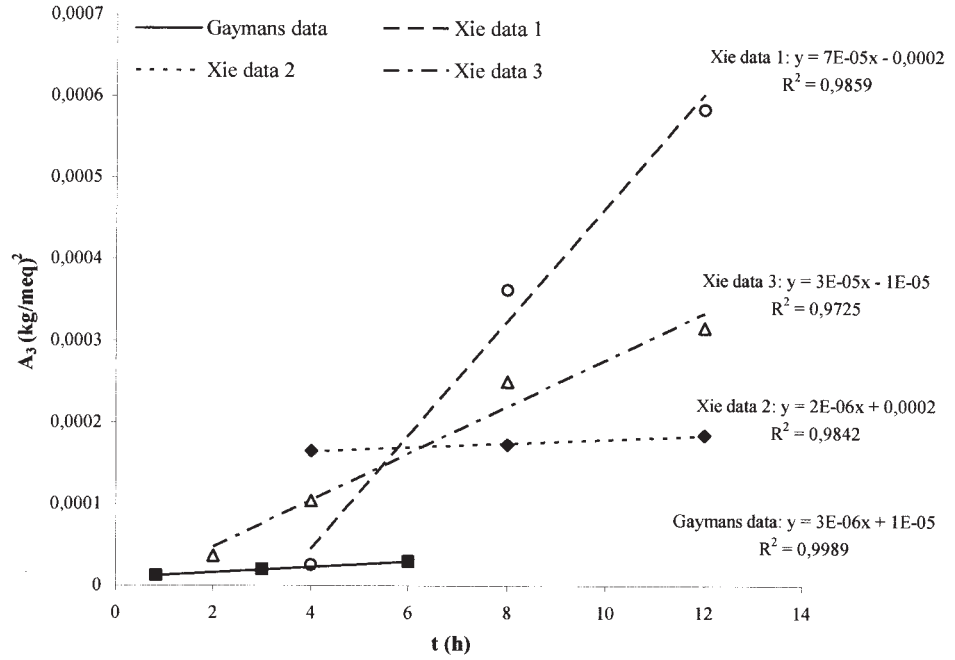

Figure 3 Fitting of rate expression A_3 to published SSP data for third-order kinetics: (■) Gaymans data (PA4,6, SSP temperature = 220°C), (○) Xie data 1 (PA6 chips with 0.03% regulator, SSP temperature = 200°C), (◆) Xie data 2 (PA6 chips, cylinder, mean diameter = 1.2 mm), and (△) Xie data 3 (PA6 chips, cylinder, mean diameter = 1.4 mm).

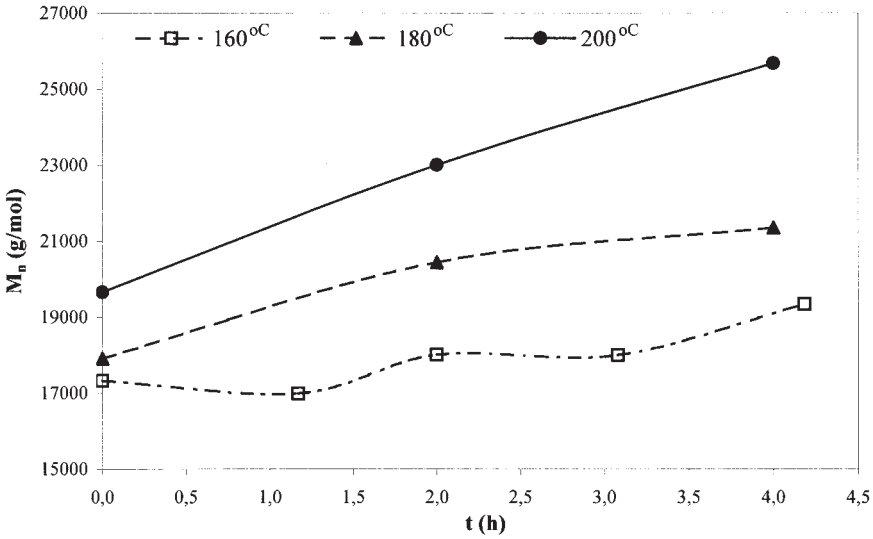

Figure 4 M_n variation during SSP at three reaction temperatures.

(>210°C), at which the chemical reaction is no longer the controlling step.[2,39,40]

PA6,6 SSP kinetics

Before studying SSP kinetics based on our data, we thought it worthwhile to examine the validity of eqs. (13) and 14 for already published SSP data of different PAs. Accordingly, the SSP data for polycaproamide (PA6) chips at 200 and 220°C (N_2: 60 mL/min) provided by Xie[14] were first used. The rate expressions A_2 (Fig. 2) and A_3 (Fig. 3) have been plotted against the reaction time, and in all cases, the proposed equations appropriately describe SSP behavior (R^2 = 0.9614–0.9859). Similarly, Gaymans's data,[16] regarding PA4,6 SSP at 220°C, were used and showed excellent fitting to the proposed model (Figs. 2 and 3; R^2 = 0.9953–0.9989).

As for our data, the results of all SSP runs are summarized in Table VI. SSP results in M_n of the prepolymer increasing by 4–31%. More specifically, M_n increases with the reaction temperature (Fig. 4) as a result of the accelerating chemical reaction, the mobility of the functional end groups, and the byproduct diffusion. The autocatalytic SSP nature is also shown because the increase in the residence time leads to a higher molecular weight as a result of allowing end groups of longer distances to approach each other and react.

On the basis of the DSC data (Table VII), the crystallinity is constant throughout SSP, and this allows the use of the kinetic expressions without consideration of the two-phase model. The SEC results show an increase in the polydispersity index (PDI) of the SSP product at higher SSP temperatures. The observed broadening of MWD is in accordance with Flory's theory,[22] which states that MWD widens during a typical linear step polymerization. Degradation reactions seem to be avoided because otherwise they would result in a narrowing of MWD.[41] Finally, when comparing SEC results (Table VII) and end-group concentrations (Tables IV and VI) with respect to the molecular weight determination, we find that the M_n values are close enough, and the low deviations reveal the reliability of the specific experimental procedures.

As for the SSP kinetics, the mean values of the rate constants for two reaction times (2 and 4 h) are presented in Table VIII, based on the second- and third-order approaches of eqs. (13) and (14) and on the Fujimoto model[33] [eq. (10), Table I], which serves as a

TABLE VII
DSC and SEC Results of PA6,6 SSP Products (t = 4 h)

	DSC			SEC		
Sample	Melting temperature (°C)	Enthalpy of fusion (ΔH) melting (cal/g)	x_c (%)	M_n (g/mol)	M_w (g/mol)	PDI
PA6,6	261.6	13.4	26	19,200	37,000	1.93
PA1604	261.0	12.6	25			
PA1804	261.2	12.8	25			
PA2004	262.0	11.8	23	30,500	69,600	2.28

TABLE VIII
Reaction Rate Constants for PA6,6 SSP

Equations (13) and (14)				
T (°C)	$100k_2$ (kg/mequiv) h^{-1}	% SDM (k_2)	$1000k_3$ (kg/mequiv)^2 h^{-1}	% SDM (k_3)
160	0.051	1	0.008	0
180	0.113	11	0.018	9
200	0.221	13	0.040	11

Equation (10)		
T (°C)	k (h^{-1})	R^2
160	5.924	0.9597
180	9.903	0.9995
200	24.968	0.9999

tool for the easy and simple monitoring of the SSP progress. Regarding the Flory-theory-based model, the second- and third-order kinetics show similar fittings, and more specifically, the third-order kinetics present slightly better fitting than the second-order kinetics. This observation has also been made during the SSP of PA6,6 fibers in the temperature range of 220–250°C.[29] In addition, the correlation coefficient in the Fujimoto model is significantly high for $n = 1$ [eq. (10)]. As expected, the rate constants increase with increasing temperature. The average SSP rate constant for the third-order kinetics increases by 63% with each 10°C increase in the temperature.

The SSP E_a value (Table IX) has been deduced from the Arrhenius plots (Fig. 5). The range of E_a values found in the literature is 10–76 kcal/mol (Table II), and the values derived here are in accordance with these limits. The observed variation in the values of E_a may be attributed to differences in the experimental conditions and in the nature of the starting material: the starting PA 6,6 resin contains no additives, and so the kinetic investigation is expected to be much more reliable. The linearity in the Arrhenius plots again verifies the validity of the selected kinetic expressions (R^2 = 0.9647–0.9998). Both models have similar E_a values (16.84 and 14.56 kcal/mol, respectively). The Arrhenius equation has been deduced for the SSP of PA6,6 in the temperature range of 160–200°C:

TABLE IX
PA6,6 SSP E_a Values

Equation (14) (third-order kinetics)		
Temperature range (°C)	E_a (kcal/mol)	A (kg/mequiv)^2 h^{-1}
160–200	16.84	2436
Equation (10)		
Temperature range (°C)	E_a (kcal/mol)	A (h^{-1})
160–200	14.56	1.23×10^8

$$k_3 = 4.8 \times 10^{-6} \exp\left(\frac{16{,}845}{R}\left(\frac{1}{423} - \frac{1}{T}\right)\right) \quad (16)$$

where T is the absolute reaction temperature (K) and R is the universal gas constant.

In summary, the simple Flory model of eqs. (13) and (14) can be used for process design and operation to describe the reaction progress. The comprehensive models usually involve a system of partial differential equations, which describe the changes with time and position of all chemical species within the reacting particle. Each species balance contains the rates of all reactions in which the species participates, and each condensate molecule balance contains an additional term for diffusion of the condensate within the particle. Equations (13) and (14) may be considered reliable rate expressions on the basis of the good fitting for both our data and data previously published, and thus they may be incorporated into comprehensive models as the determination of the apparent rate constants becomes feasible.

CONCLUSIONS

SSP of PA6,6 has been carried out under nitrogen in the temperature range of 160–200°C. The fitting of the experimental data to SSP kinetic models proposed already has been investigated, and a rate expression based on Flory's equations has been used. The latter has been satisfactorily tested for the SSP of PAs under various conditions. It fits end-group-based SSP data very well, and so it is adequate to describe SSP behavior. Reaction rate constants and SSP E_a values have been derived, and they can be used in the comprehensive SSP models, instead of these values being extrapolated from melt data. Finally, on the basis of this kinetic analysis, a comparison during SSP of different PA compositions is feasible, especially when modifiers are incorporated into the PA structure.

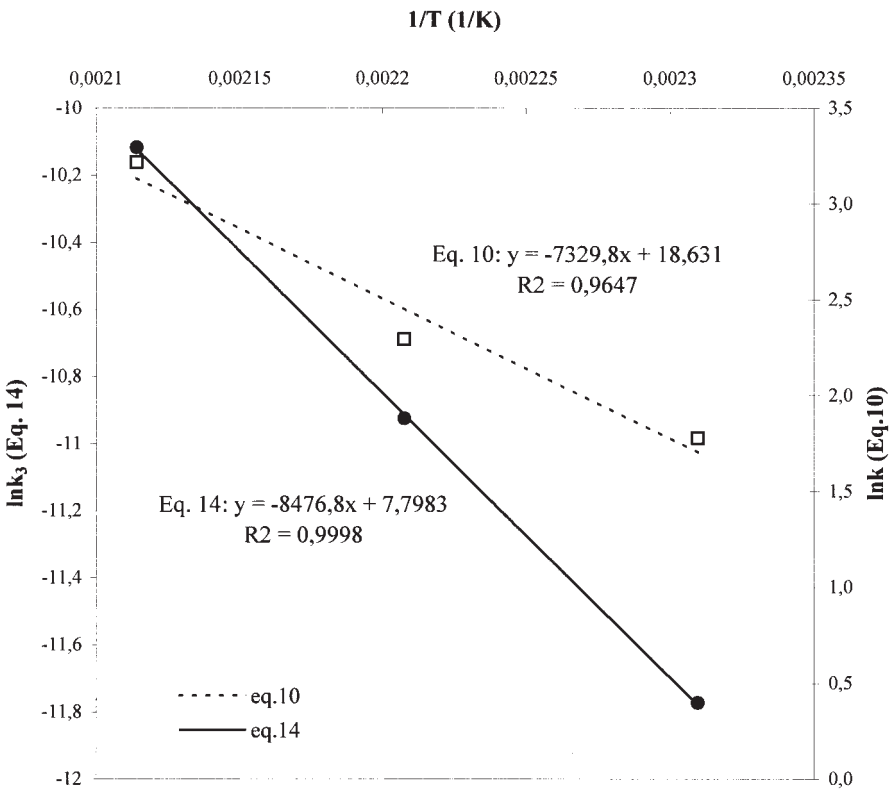

Figure 5 Arrhenius plots based (●) on third-order kinetics [eq. (14)] and (□) on the Fujimoto model [eq. (10)].

The authors thank Simone Arizzi for his solid support during the ongoing research project between the National Technical University of Athens and INVISTA, Inc., and P. Hytrek for the reactor assembly and operation instructions.

References

1. Dujari, R.; Cramer, G.; Marks, D. W.O. Pat. 98/23666 (1998).
2. Kim, T.; Lofgren, E.; Jabarin, S. J Appl Polym Sci 2003, 89, 197.
3. Flory, P. U.S. Pat. 2,172,374 (1939).
4. Monroe, G. U.S. Pat. 3,031,433 (1962).
5. Papaspyrides, C. In The Polymeric Materials Encyclopedia; Salamone, J. C., Ed.; CRC: Boca Raton, FL, 1996; p 7819.
6. Papaspyrides, C. Polym Int 1992, 29, 293.
7. Papaspyrides, C. Polymer 1988, 29, 114.
8. Ravindranath, K.; Mashelkar, R. J Appl Polym Sci 1990, 39, 1325.
9. Heinz, H.; Schulte, H.; Buysch, H. Eur. Pat. 410,230/91 A2 (1991).
10. Weger, F.; Hagen, R. U.S. Pat. 5,773,555 (1998).
11. Gross, S.; Roberts, G.; Kiserow, D.; DeSimone, J. Macromolecules 2000, 33, 40.
12. Zimmerman, J. Polym Lett 1964, 2, 955.
13. Zimmerman, J.; Kohan, M. J Polym Sci Part A: Polym Chem 2001, 39, 2565.
14. Xie, J. J Appl Polym Sci 2002, 84, 616.
15. Duh, B. J Appl Polym Sci 2002, 84, 857.
16. Gaymans, R. In Polymerization Reactors and Processes; Henderson, J. N.; Schuijer, J.; Bouton, C. T., Eds.; ACS Symposium Series; American Chemical Society: Washington, DC, 1979, 104, pp 137–148.
17. Goodner, M.; DeSimone, J.; Kiserow, D.; Roberts, G. Ind Eng Chem Res 2000, 39, 2797.
18. Huang, B.; Walsh, J. Polymer 1998, 39, 6991.
19. Gaymans, R.; Amirtharaj, J.; Kamp, H. 1982, 27, 2513.
20. Wu, D.; Chen, F.; Li, R.; Shi, Y. Macromolecules 1997, 30, 6737.
21. Yao, Z.; Ray, W. AIChE J 2001, 47, 401.
22. Flory, P. Principles of Polymer Chemistry; Cornell University Press: Ithaca, NY, 1975; pp 75 and 317.
23. Secor, R. AIChE J 1969, 15, 861.
24. Srinivasan, R.; Desai, P.; Abhiraman, A.; Knorr, R. J Appl Polym Sci 1994, 53, 1731.
25. Jabarin, S.; Lofgren, E. J Appl Polym Sci 1986, 32, 5315.
26. Duh, B. J Appl Polym Sci 2001, 81, 1748.
27. Li, L.; Huang, N.; Liu, Z.; Tang, Z.; Yung, W. Polym Adv Technol 2000, 11, 242.
28. Mallon, F.; Ray, W. J Appl Polym Sci 1998, 69, 1233.
29. Srinivasan, R.; Almonacil, C.; Narayan, S.; Desai, P.; Abhiraman, A. Macromolecules 1998, 31, 6813.
30. Kim, T.; Jabarin, S. J Appl Polym Sci 2003, 89, 213.
31. Walas, S. Reaction Kinetics for Chemical Engineers; McGraw-Hill: New York, 1959; p 126.
32. Griskey, R.; Lee, B. J Appl Polym Sci 1966, 10, 105.
33. Fujimoto, A.; Mori, T.; Hiruta, S. Nippon Kagaku Kaishi 1988, No. 3, 337.
34. Chen, F.; Griskey, R.; Beyer, G. AIChE J 1969, 15, 680.
35. Shi, C.; DeSimone, J.; Kiserow, D.; Roberts, G. Macromolecules 2001, 34, 7744.
36. Chen, S.; Chen, F. J Polym Sci Part A: Polym Chem 1987, 25, 533.
37. Shi, C.; Gross, S.; DeSimone, J.; Kiserow, D.; Roberts, G. Macromolecules 2001, 34, 2062.
38. Ma, Y.; Agarwal, U.; Sikkema, P.; Lemstra, P. Polymer 2003, 44, 4085.
39. Chang, T. Polym Eng Sci 1970, 10, 364.
40. Chang, C.; Sheu, M.; Chen, S. J Appl Polym Sci 1983, 28, 3289.
41. Korshak, V.; Frunze, T. Synthetic Hetero-Chain Polyamides; Israel Program for Scientific Translations: Jerusalem, 1964; pp 87 and 442.